^{1}H NMR Studies on the Reorientational Motions of Cations in Four Solid Phases of Methylammonium Iodide and the Self-Diffusion of Ions in Its Highest-Temperature Solid Phase

Hiroyuki Ishida, Ryuichi Ikeda, and Daiyu Nakamura*
Department of Chemistry, Faculty of Science, Nagoya University,
Chikusa-ku, Nagoya 464
(Received September 20, 1985)

Four solid phases of CH_3NH_3I named as α', β', δ, and ε were studied by the temperature dependence of ^{1}H spin-lattice relaxation time T_1 and ^{1}H spin–spin relaxation time T_2 (for ε) at several NMR frequencies, and of ^{1}H NMR second moment. Phase transitions were studied by means of differential thermal analysis and ^{1}H T_1. The X-ray powder patterns of the highest-temperature ε phase taken at ca. 440 K revealed that the crystal forms a CsCl-type cubic lattice. The measurements of differential scanning calorimetry gave unusually small entropy of melting indicating that the cations of the ε phase are in a state having the most part of their motional freedom. From ^{1}H NMR T_1 experiments, it was found that the transformation of the room-temperature α' phase to the low-temperature stable β' phase needed longer time than three months at Dry Ice temperature for samples carefully purified and dried for a long time under vacuum whereas it was completed within two weeks for roughly dried samples. The NMR results indicated that the cations are bound tightly in the β' phase whereas they are fairly free to reorient in the low-temperature substable δ phase. In the α' phase, the cations perform C_3 reorientations very rapidly about their C–N bond axis. The cations of the ε phase undergo overall rotation as well as self-diffusion which was confirmed by electrical conductivity measurements. The mechanism of the self-diffusion of the cations is discussed.

Methylammonium iodide (MAI) had been known for a long time to form two solid phases below room temperature from the temperature dependence study of infrared spectra.[1,2] The α' phase stable at room temperature has a tetragonal structure belonging to the space group $P4/nmm$, and is isomorphous with the room-temperature α' phase of CH_3NH_3Br.[3] The low-temperature δ phase of MAI has been thought to have the same crystal structure as the substable δ phase of the bromide, because the two phases showed very similar IR spectra.[1,2] Recently, the transition temperature T_{tr} between the α' and δ phases of MAI was determined to be 167 K from the ^{127}I NQR study.[4]

^{1}H NMR studies on the molecular motion of the cation[5,6] were reported for MAI and its partially deuterated analog CH_3ND_3I. Recently, we found the existence of a new high-temperature ε phase stable above 414 K for MAI and reported as a letter.[5] The new phase has a marked feature that the cations undergo self-diffusion as well as overall reorientation in the crystal. In view of the dynamical behavior of ions, this phase is thought to be analogous to the high-temperature phase of $CH_3NH_3NO_3$ ($MANO_3$), which is very close to the plastic phase found in various molecular crystals.[7,8]

Very recently, Yamamuro et al.[9] found the stable low-temperature phase named as β' from the calorimetric study of MAI crystals. This phase was obtained by annealing the sample at 205 K for ca. 5 d.

In the present investigation, we have carried out measurements on the 2nd moment M_2 of ^{1}H NMR absorptions, ^{1}H spin-lattice and spin–spin relaxation times T_1 and T_2, respectively, differential thermal analysis (DTA), differential scanning calorimetry (DSC), and X-ray powder diffraction of MAI, to obtain information about the nature of the liquid-like ε phase and also to compare the dynamical properties of the cation in the stable low-temperature β' phase with those in the α' and δ phases.

Experimental

Methylammonium iodide was synthesized by mixing an aqueous solution of methylamine with a nearly stoichiometrical amount of hydroiodic acid. The resulting solution was left to stand over phosphorus pentaoxide in a vacuum desiccator to evaporate water slowly. Pale yellow crystals separated were purified by recrystallizations three times from a mixed solvent of ethanol and chloroform. Colorless tabular crystals obtained were dried in a vacuum desiccator. The partially deuterated analog, CH_3ND_3I was prepared from purified MAI by performing successive crystallizations from heavy water. All the manipulations were carried out in a dry bag because the samples were hygroscopic. After the samples were ground and put in glass ampoules, they were again dried under vacuum at ca. 80 °C.

Temperature dependence measurements of wide-line ^{1}H NMR spectra were performed at a Larmor frequency of 40 MHz by means of JEOL-MW-40S spectrometer equipped with a temperature controller. ^{1}H T_1 observed at 11.5, 20, 31.5, and 42.5 MHz was measured by the inversion recovery method using two spectrometers described elsewhere.[10,11] ^{1}H T_2 was determined at 31.5 and 42.5 MHz by applying Hahn's spin-echo method.[12] Electrical conductivity and DTA measurements were carried out by use of homemade apparatus already reported.[8,13] A Perkin-Elmer DSC-1B apparatus was used to determine enthalpy changes at the solid–solid phase transition and melting temperatures abbreviated as T_{tr} and T_m, respectively. Observed transition enthalpies were calibrated by the melting enthalpy of

metallic indium[14] (purity: 99.99%). X-Ray powder diffraction photographs were taken for the ε phase with the sample sealed in a glass capillary, using a Weisenberg camera from Rigaku Denki Co.

Results

Structural information about the ε phase was obtained by taking X-ray powder photographs at ca. 440 K. The observed patterns were well explained with a CsCl-type cubic lattice having the lattice constant a=4.86 Å and Z=1. Table 1 shows the adequacy of the present analysis.

The DTA curves recorded in a temperature range of 80-520 K were shown in Fig. 1. When the sample was heated and cooled, a small heat anomaly accompanying a long tail on the low-temperature side was observed at the same peak-temperature of 167 K. As already reported for the phase transitions

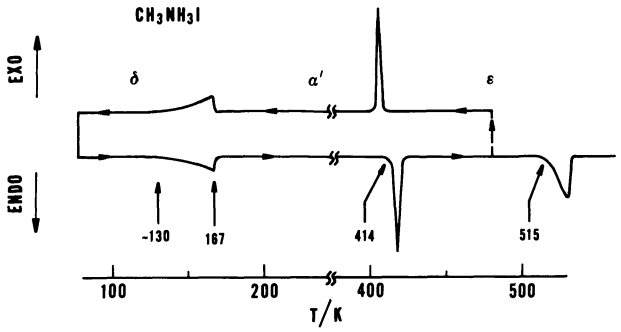

Fig. 1. Differential thermal analysis (DTA) curves of CH_3NH_3I crystals. Endothermic anomalies due to solid-solid phase transitions from the low-temperature substable δ to the room-temperature α' phase and from α' to the highest-temperature solid phase ε appear at 167 and 414 K, respectively. Heat anomaly due to phase transition between the low-temperature stable β' phase and α' is missing.

Table 1. Comparisons between Observed and Calculated 2θ Values of X-Ray Diffraction Patterns Taken at ca. 440 K for CH_3NH_3I, (Cubic, a=4.86 Å)

Index	2θ/degree	
hkl	Obsd	Calcd
100	18.4	18.3
110	26.0	25.9
111	31.9	31.9
200	37.0	37.0
210	41.5	41.6
211	45.5	45.7
220	53.2	53.3
300	56.6	56.8
310	60.0	60.2

taking place in some methylammonium salts[13,15,16] which showed small heat anomalies similar to the above one, the temperature of the DTA peak could be attributed to T_{tr} (167 K). This agrees well with T_{tr} determined for this salt from the temperature dependence study of ^{127}I NQR[4] and that (166.1 K) from the heat capacity study.[9]

When the sample was heated above room temperature, a large heat-absorption anomaly was recorded at 414 K. The enthalpy change at this phase transition was determined from DSC measurements as 6.1 kJ mol^{-1}. With increasing temperature furthermore, melting of the sample started at ca. 515 K together with gradual decomposition which was confirmed by observing the color change to yellow. The enthalpy of melting was roughly estimated to be ca. 7 kJ mol^{-1}.

In CH_3ND_3I, a heat anomaly was observed at the same temperature of 167 K as that of MAI, having almost the same shape as that of MAI recorded on the DTA measurements of both heating and cooling runs. On the other hand, the phase transition to the ε phase took place at 419 K which is higher by 5 K than that of MAI.

The samples used in the foregoing DTA experiments were dried by keeping the glass tubes at 80 °C for ca. 8 h under a high vacuum in order to remove an extremely small amount of water and other volatile impurities possibly included in them. These samples were only partly transformed in our experiments from α' into the low-temperature stable β' phase found by Yamamuro et al[9] although they were left to stand (annealed) for three months at the Dry Ice temperature (196 K). The existence ratio of β' to α' phase was determined at ca. 196 K by separating free induction decay signals of these phases which gave greatly different T_1 of 10 ms and 10 s, respectively. For the above samples repeatedly prepared several times, the β'-phase content was observed to be in a range of ca. 70—0% after the foregoing annealing treatment. These variations of the content values may be due to impurities included in the sample and/or the difference of the grain size of the pulverized crystals. On the other hand, the samples dried at room temperature for ca. 20 min under a high vacuum were transformed into the β' phase almost completely, even when they were annealed at the same temperature only for two weeks. Accordingly, the samples dried by the former method were employed for the ^1H NMR measurements of the α', δ, and ε phases and also for the DTA and DSC experiments, while those dried by the latter method were employed for the study of ^1H NMR only for the β' phase.

The temperature variation of M_2 observed for MAI between 77 and 430 K is shown in Fig. 2. An almost temperature independent M_2 of ca. 8.5 G^2 was

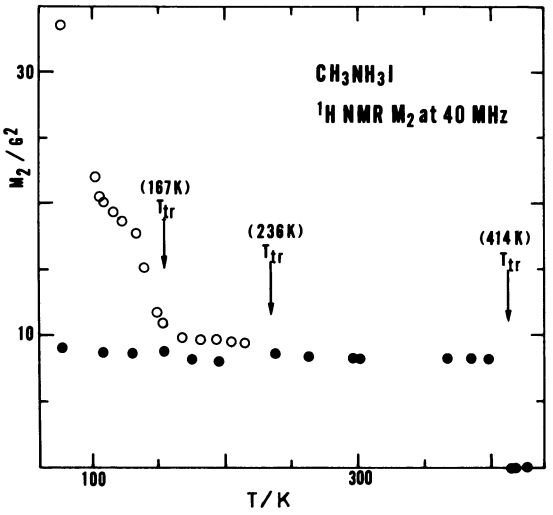

Fig. 2. Proton NMR second moment, M_2 observed at a Larmor frequency of 40 MHz for CH_3NH_3I crystals (○ for β': ● for α', δ, and ε). The transition temperature, T_{tr} from β' to α' was determined from ^1H T_1 experiments as 236 K while other T_{tr} values from DTA.

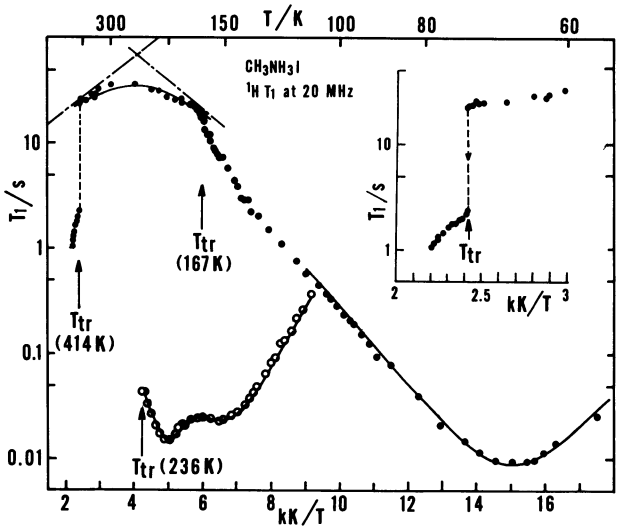

Fig. 3. Temperature dependences of ^1H T_1 observed at 20 MHz for CH_3NH_3I. T_1 data obtained for the α', δ, and ε phases are shown by dots while those of β' phase are plotted by open circles. The enlarged plots near T_{tr} from α' to ε are inserted. Solid curves indicate best fitted curves calculated by the least-squares method. Solid lines broken by dots given in the α' phase are the calculated log T_{1MA} and log T_{1SR} lines defined in the text.

obtained for the α' phase below ca. 410 K and also for the δ phase above 77 K. The M_2 values of 8.8 and 7.5 G^2 determined at 77 and 300 K, respectively, by Tsau and Gilson[17] are consistent with the present results. The large M_2 value of 34±3 G^2 was obtained at 77 K for the β' phase. With increasing temperature, M_2 of this phase decreased gradually and an almost constant value of 9.5±0.3 G^2 was observed between 170 and 220 K, above which temperature we could not definitely discriminate between the β' and α' phases because of the coexistence of both phases. When the sample was heated from room temperature, M_2 decreased discontinuously at T_{tr} to the ε phase and extraordinarily small M_2 values less than 0.01 G^2 were obtained for this phase.

The temperature dependences of ^1H T_1 in MAI and CH_3ND_3I determined in a temperature range of 57—455 K at 20 MHz are shown in Figs. 3 and 4, respectively.

The δ phase of MAI and CH_3ND_3I exhibited a single T_1 minimum the value of which was 9 and 12 ms, respectively, at approximately the same temperature of 67 K. With increasing temperature in this phase up to ca. 130 K, the log T_1 versus T^{-1} plot increased linearly. Above 130 K, the log T_1 value increased more steeply and deviated from a line obtained by extrapolation from the low-temperature side. Moreover, a small jump in the log T_1 curve could be found at 167 K. This temperature agrees well with T_{tr} determined by DTA. By referring to the anomalous DTA curve observed around T_{tr}, this transition is attributable to a second-order one.

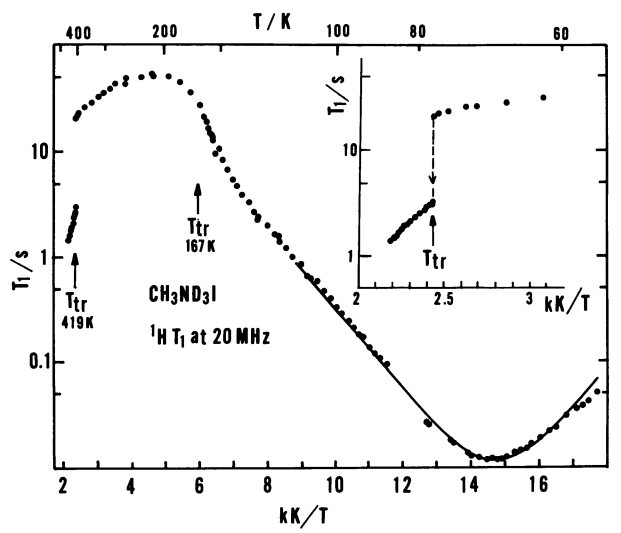

Fig. 4. Temperature dependences of ^1H T_1 observed at 20 MHz for CH_3ND_3I. Near T_{tr} from the α' to ε phase, the axis of abscissa is enlarged and an enlarged plot is inserted in the figure. The solid curve is the best-fitted theoretical curve.

However, a slight discontinuity in T_1 was observed at T_{tr} suggesting the presence of some first-order nature in this phase transition.

In the β' phase of MAI, two T_1 minima of 22 and 15 ms were located at 154 and 202 K, respectively. At 236 K, T_1 increased discontinuously by about two

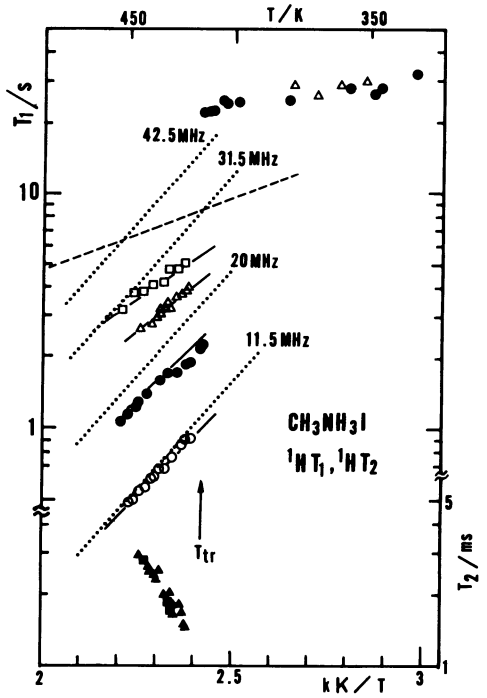

Fig. 5. Temperature dependences of ^1H T_1 observed at 11.5 (○) 20 (●), 31.5 (△), and 42.5 (□) MHz; and ^1H T_2 observed at 31.5 (▲) and 42.5 (■) MHz mainly for the ε phase of CH_3NH_3I. The frequency independent $\log T_{1l}$ estimated for the ε phase is shown by a broken line and frequency dependent $\log T_{1d}$ derived from each observed frequency is shown by dotted lines. Solid lines indicate the best fitted one to the observed values at each frequency.

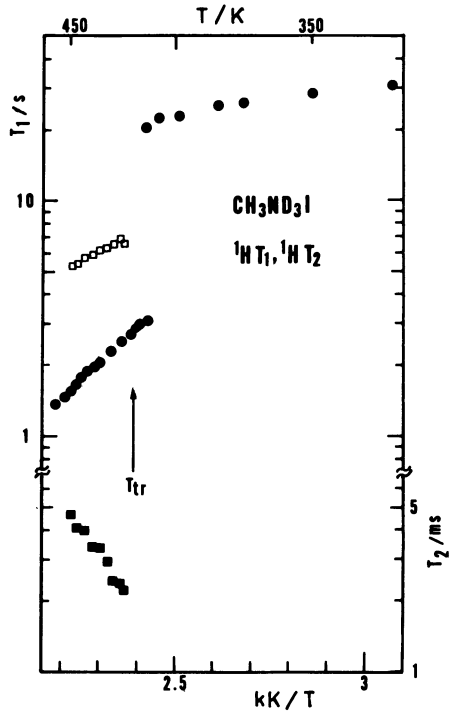

Fig. 6. Temperature dependences of ^1H T_1 observed at 20 (●) and 42.5 MHz (□); and ^1H T_2 observed at 42.5 MHz (■) mainly for the ε phase of CH_3ND_3I.

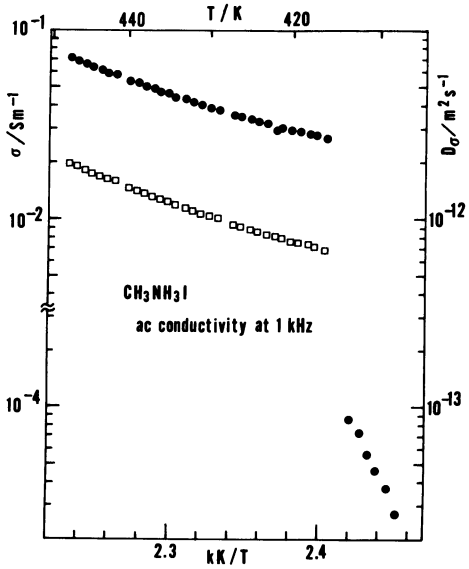

Fig. 7. Temperature dependences of electrical conductivity σ (●) values observed at 1 kHz and the diffusion constants D_σ (□) evaluated for CH_3NH_3I.

orders of magnitude, above which temperature the same T_1 values as those of the α' phase were observed. Accordingly, this discontinuity observed in T_1 can be assigned to the phase transformation from β' to α'. The transformation was completed with a reasonably fast rate at this temperature which is higher than T_{tr} of 220 K determined from the calorimetric study,[9] where superheating of β' by ca. 10 K was reported.

In the α' phase of MAI, a broad T_1 maximum (ca. 35 s) was observed at ca. 270 K. A similar maximum of ca. 40 s was also obtained at ca. 240 K for the α' phase of CH_3ND_3I. With increasing temperature, a sudden T_1 decrease was observed for the α' phase of MAI and CH_3ND_3I at 414 and 419 K, respectively. These temperatures agree well with T_{tr} to the ε phase already determined by DTA.

The temperature dependences of ^1H NMR relaxation times (T_1, T_2) determined for each ε phase of MAI and CH_3ND_3I are given in Figs. 5 and 6, respectively.

In each ε phase, plots of $\log T_1$ decreased linearly with decreasing T^{-1}, whereas those of $\log T_2$ increased linearly against T^{-1}.

Electrical conductivity measurements were performed for pulverized MAI crystals by use of 1 kHz ac electric field in a temperature range of 408—443 K and the results are shown in Fig. 7. When the sample was heated in the α' phase, the electrical conductivity σ increased steeply but continuously. However, it jumped at T_{tr} to the value of 2.7×10^{-2} S m^{-1}, which is larger by about three orders of magnitude than those obtained for the α' phase.

Discussion

Calculated Second Moments. Theoretical values of M_2 for a MA^+ ion in the following three motional states were evaluated by assuming the same geometry of the cation as that employed in our previous report on solid CH_3NH_3Br.[16] The M_2 values calculated for the cation, in the rigid lattice, performing the reorientation as a whole about the cationic C_3 axis, and undergoing the overall rotation about its center of gravity. They are 38, 11, and 1.1 G^2, respectively. ^1H–^1H and ^1H–^{127}I interionic contributions to M_2 were estimated by use of the crystal structure of the α' phase[3] for the calculations of the first two cationic motional states. For the ε phase revealed in the present investigation, M_2 was calculated for the last motional state because the cation should behave as an isotropic ion in the cubic ε phase.

Low-Temperature Substable δ Phase. The M_2 value of 8.5 G^2 observed for the δ phase is close to the value calculated for the cation in which both CH_3 and NH_3^+ groups perform C_3 reorientation about their symmetry axis. From this value, the averaged reorientational rates of both groups can be estimated to be faster than 10^5 Hz in the δ phase above 77 K.

The random C_3 reorientation of either CH_3 or NH_3^+ group gives rise to ^1H T_1 expressed by,[18]

$$T_1^{-1} = C\{\tau_R/(1+\omega_H^2\tau_R^2) + 4\tau_R/(1+4\omega_H^2\tau_R^2)\}, \quad (1)$$

where

$$C = (9/20)\gamma_H^4\hbar^2 r^{-6}. \quad (2)$$

In these equations, γ_H, r, ω_H, and τ_R are the gyromagnetic ratio of a proton, the interprotonic distance, the ^1H angular Larmor frequency, and the correlation time of either CH_3 or NH_3^+ C_3 reorientation, respectively. Taking into account only for each intragroup contribution to the relaxation, the spin-lattice relaxation rate, T_{1MA}^{-1} of the cations can be written as,

$$T_{1MA}^{-1} = (1/2)(T_{1CH_3}^{-1} + T_{1NH_3}^{-1}), \quad (3)$$

where T_{1CH_3} and T_{1NH_3} are given by Eq. 1.

The T_1 minima of 9 and 12 ms observed for the δ phase of MAI and CH_3ND_3I, respectively, agree well with the theoretical values of 9.9 and 11 ms in the same order. These values were calculated by use of Eqs. 1—3 for the C_3 reorientations of CH_3 and NH_3^+ groups in MAI crystals and for the C_3 reorientation of CH_3 groups in CH_3ND_3I crystals. In this calculation, we employed the same geometry of the cation as that used in the calculation of M_2.

Assuming an Arrhenius-type relationship between the activation energy, E_a for the C_3 reorientation and τ_R, we have

$$\tau_R = \tau_{RO}\exp(E_a/RT), \quad (4)$$

where τ_{RO} has the usual meaning. Fitting calculation of the ^1H T_1 data of MAI and CH_3ND_3I determined in the δ phase to Eqs. 1—4 was performed by the least-squares method using a program SALS[19] in the Computation Center of Nagoya University. The best fitted T_1 curves obtained are shown in Figs. 3 and 4 by solid lines. The optimum values of E_a, τ_{RO}, and C obtained through the calculation are given in Table 2.

The motional mode of the cation in the δ phase of MAI and CH_3ND_3I can be considered from the following discussion as the C_3 reorientation of the cation as a whole with keeping its rigid structure. This motional mode (correlated C_3 reorientation) of the cation has already been observed in some hexahalo metal complexes.[20,21] The presence of the correlated C_3 reorientation of the cation in the δ phase is explained by the facts that MAI gives a single T_1 minimum attributable to the C_3 reorientation of both CH_3 and NH_3^+ groups, and the E_a value of ca. 7 kJ mol^{-1} obtained for both salts is smaller than that of ca. 8 kJ mol^{-1} evaluated for the barrier to internal rotation of the cation.[20,21] The appearance of this motional mode indicates that the cations are considerably free to reorient about their C–N bond axes and, therefore, the δ phase forms loosely packed crystals.

Above 133 K, ^1H T_1 observed for MAI deviated gradually from the calculated curve. The deviation of T_1 from the normal BPP curve far below T_{tr} and the anomalous DTA curve recorded in the same temperature region have been also observed below T_{tr} from the δ to α' phase of CH_3NH_3Br crystals.[16] This T_1 deviation can be regarded as a significant feature of the second-order-like phase transition from the substable δ phase to the room-temperature α' phase. Therefore, it is expected that the correlation time of the C_3 reorientation of the cation in these crystals is shortened rapidly near T_{tr} with increasing temperature.

Low-Temperature Stable β' Phase. By comparing M_2 of 34±3 G^2 observed at 77 K in the β' phase with the theoretical value of 38 G^2 for the rigid lattice, the cations can be expected to be almost rigid in the crystal. This is in a marked contrast to the motional state of the cation in the δ phase described above and indicates that the cations in the β' phase are strongly hindered to reorient. Accordingly, one can conclude that the ions in the β' phase are more compactly packed in crystals than those of δ in accordance with the fact that the former phase rather than the latter is the stable one at low temperatures.[9]

The ^1H T_1 data of these phases are capable of a similar interpretation. A shallow T_1 minimum of

Table 2. Activation Energies (E_a), Pre-Exponential Factors (τ_{RO}), Motional Constants (C), and Motional Modes of Methylammonium Ions in Four Phases of Solid Methylammonium Iodide

	Phase	E_a/kJ mol^{-1}	$\tau_{RO}/10^{-14}$ s	$C/10^9$ s^{-2}	Motional Mode
CH_3NH_3I	δ	6.6±0.1	2.7	9.8	Correlated C_3 reorient.
	β'	11.2±0.1	73	7.3	C_3 reorient. of CH_3
		22.1±0.4	1.1	9.6	C_3 reorient. of NH_3^+
	α'	5±1			C_3 reorient. of CH_3 and NH_3^+
	ε	35±5 (48±3)*			Self-diffusion
CH_3ND_3I	δ	7.2±0.1	1.3	7.6	Correlated C_3 reorient.
	ε	(45±3)*			Self-diffusion

*Evaluated from T_2.

22 ms appearing at the lower temperature of 154 K in the β' phase of MAI can be assigned to the CH_3 C_3 reorientation, while the deep one (15 ms) at 202 K is attributable to the NH_3^+ C_3 reorientation in agreement with the temperature dependence of M_2 observed in this phase. These assignments of ^1H T_1 minima are acceptable because ^1H T_1 minima calculated for CH_3 and NH_3^+ groups performing the C_3 reorientation in the cation are 23 and 17 ms, respectively, at a Larmor frequency of 20 MHz.[20] The motional parameters and activation energies for the C_3 reorientation of both groups were evaluated in the same way as that described in the foregoing δ phase. The results are given in Table 2 and the calculated curve is shown in Fig. 3 by solid line. The E_a values obtained for the C_3 reorientation of both groups are larger in β' than in δ clearly indicating that the cations in the former phase are more tightly bound in the crystalline lattice in agreement with the foregoing discussion.

It is noteworthy that the β' crystal of MAI yields two ^1H T_1 minima while the δ only a single minimum. This indicates that the correlated C_3 reorientation of the cation is the easiest reorientational mode of the cation in the latter crystal, whereas the barrier of the CH_3 groups to reorient in the former, which is considerably higher than that of the internal rotation, is distinguishably lower enough than that of the NH_3^+ groups. The large E_a value derived for the NH_3^+ C_3 reorientation in β' suggests that this phase has a crystal structure efficiently to be formed by N–H···I type hydrogen bonds.

Room-Temperature α' Phase. In this phase, a ^1H T_1 maximum was observed for both MAI and CH_3ND_3I crystals, and it should be noted that no frequency dependence was observed in the hot side of the maximum. These experimental facts indicate that a new relaxation process other than the usual magnetic dipolar relaxation contributes to ^1H T_1 observed in this phase. The most feasible mechanism for the new motional process is spin-rotation relaxation originating from the uniaxial rotation of the CH_3 and NH_3^+ groups around each C–N bond axis of the cations. For the crystals of several ammonium salts,[22–24] where NH_4^+ ions are thought to be almost free to perform overall rotation, it is reported that ^1H T_1 can be interpreted in terms of this mechanism. Although the present cation performs uniaxial reorientation in the crystal, this process is still valid provided that the reorientation is rapid enough.

When both spin-rotation and magnetic dipolar interactions due to the uniaxial rotation of the cations contribute to ^1H T_1, the observed T_1 can be written by

$$T_1^{-1} = T_{1MA}^{-1} + T_{1SR}^{-1}, \tag{5}$$

where T_{1SR} indicates ^1H T_1 originating from the spin-rotation mechanism. Since the condition, $\omega_H\tau_R \ll 1$ is fulfilled for both CH_3 and NH_3^+ reorientations in the α' phase, T_{1MA} can be connected with the averaged C_3 reorientational correlation time $\bar{\tau}_R$ of these groups by,

$$T_{1MA}^{-1} = (5/2)(C_{CH_3} + C_{NH_3^+})\bar{\tau}_R, \tag{6}$$

where C_{CH_3} and $C_{NH_3^+}$ denote the motional constants for the CH_3 and NH_3^+ C_3 reorientations, respectively, as given in Eq. 2. Therefore, log T_{1MA} is expected to increase linearly with decreasing T^{-1} in this phase because $\bar{\tau}_R$ can be expressed by Eq. 4.

For T_{1SR}, a temperature dependence can be derived from a theoretical consideration that T_{1SR} is propor-

tional to $\bar{\tau}_R$ in the present system.[25] Under a condition that both $\log T_{1MA}$ and $\log T_{1SR}$ change linearly against T^{-1}, the T_1 data observed can be divided into two components by the least-squares method. The best fitted T_{1MA} and T_{1SR} straight lines thus obtained are shown in Fig. 3 using solid lines broken by dots. The gradient of the two lines having opposite signs yielded the same E_a of 5 ± 1 kJ mol^{-1}. This result is compatible with our present assumptions that both T_{1MA}^{-1} and T_{1SR} are proportional to $\bar{\tau}_R$.

Since the present E_a obtained for the C_3 reorientation of the cation is comparable to the thermal energy at 300 K ($RT\approx2.5$ kJ mol^{-1}), we can say that the cations perform the C_3 reorientation quite freely in this phase. This provides a strong support for the presence of the spin-rotation relaxation. Substituting the value of $(C_{CH_3}+C_{NH_3^+})$ calculated using Eq. 2 into Eq. 6, one obtains $\bar{\tau}_R$ to be 1.5×10^{-13} s at 300 K. This is extraordinarily short for usual solids and nearly the same order of magnitude as those usually observed for nonviscous liquids. For example, $\bar{\tau}_R$ for the C_3 rotation of CH_3 groups in liquid toluene is reported to be ca. 1×10^{-13} s at ca. 250 K,[26] and that for the overall rotation of molecules in liquid ammonia is ca. 2×10^{-13} s at 347 K.[27] ^{1}H T_1 observed for these compounds in their liquid state is reported to clearly involve the spin-rotation mechanism. Therefore, it may be concluded that the spin-rotation relaxation due to highly free uniaxial-rotation of the present cations plays an important role in ^{1}H T_1 observed at elevated temperatures.

High-Temperature ε Phase. The extremely small M_2 and unusually long T_2 values observed for this phase imply that the isotropic rotation of the cation about its center of gravity and also self-diffusion of the cations in the crystal take place rapidly. As reported previously for the highest-temperature solid phase of $CH_3NH_3NO_3$[7,8] the most effective relaxation mechanism in the ε phase of the present salt is expected to be the cationic self-diffusion.

In the present ε phase, MA^+ cations perform isotropic reorientations which are assumed to occur much more frequently than the translational jump of the cation through the lattice sites. This means that we can calculate average distances between protons belonging to different cations by simply regarding as that the all protons in a cation are fictitiously located at the center of gravity of the cation.

In our previous study,[8] we employed the monovacancy mechanism for the explanation of the cationic self-diffusion in crystals as a simple mechanism and could well explain the observed NMR data. According to Torrey and Sholl,[28,29] the ^{1}H spin-lattice relaxation rate, T_{1HH}^{-1} and the ^{1}H spin-spin relaxation rate, T_{2HH}^{-1} due to interionic ^{1}H dipolar interactions which are randomly modulated by self-diffusion can be written by,

$$T_{1HH}^{-1}=2\alpha y[g(y)+4g(2y)], \tag{7}$$

$$T_{2HH}^{-1}=\alpha y[3g(0)+5g(y)+2g(2y)], \tag{8}$$

where

$$\alpha=(3/20)\gamma_H^4\hbar^2pa^{-6}\omega_H^{-1}, \tag{9}$$

$$y=(1/2)\omega_H\tau_H. \tag{10}$$

In the above equation, a, p, and τ_H are the lattice constant, the ratio of the number of the resonant protons to the number of the lattice sites in a unit sublattice, and the correlation time of the self-diffusion of the cations respectively. The detailed expression of $g(y)$ is given in Sholl's paper.[29]

Besides magnetic dipolar interactions operative between protons, interactions between protons and iodine nuclei also provide another relaxation process, because iodine nuclei having a large quadrupole moment are expected to have a shorter relaxation time than T_{1HH} due to appreciably fast quadrupolar relaxation even if the crystal has high symmetry such as cubic. In fact, the iodine nuclei in the crystals of the high-temperature phases of NH_4I having CsCl and NaCl type cubic structures are known to have the temperature independent T_1 of ca. 3.2 ms.[30] Under the assumption of shorter ^{127}I T_1, the relaxation times T_{1HI} and T_{2HI} can be expressed by,[18,29]

$$T_{1HI}^{-1}=2\beta\tau_H[g'\{(\omega_H-\omega_I)\tau_H\}+3g'(\omega_H\tau_H)+6g'\{(\omega_H+\omega_I)\tau_H\}], \tag{11}$$

$$T_{2HI}^{-1}=\beta\tau_H[2g'(0)+g'\{(\omega_H-\omega_I)\tau_H\}+3g'(\omega_H\tau_H)+6g'(\omega_I\tau_H)+6g'\{(\omega_H+\omega_I)\tau_H\}], \tag{12}$$

where

$$\beta=(7/12)\gamma_H^2\gamma_I^2\hbar^2a^{-6}. \tag{13}$$

In these equations, γ_I and ω_I denote the gyromagnetic ratio and the angular resonance frequency of ^{127}I nuclei, respectively. The functional form of $g'(y)$ is the same as that of $g(y)$, where the positional vectors connecting protons are replaced by those connecting ^{1}H and ^{127}I nuclei for the former function.

As another relaxation mechanism between ^{1}H and ^{127}I nuclei, the dipolar relaxation of the second kind proposed by Norris et al.[31] is expected to contribute to ^{1}H T_1 because T_1 of the quadrupolar ^{127}I nuclei is considered to become very short as in the case reported for NH_4I.[30] Since no data of the relaxation times of ^{127}I in any phase of solid MAI are available, we roughly estimated the T_1 value of MAI due to this mechanism. The calculation was performed by use of the equation reported by Norris et al.[31]

assuming the same ^{127}I T_1 value as that of NH_4I described above. The T_1 value evaluated is longer by ca. 10^4 times than the values observed in this phase. This suggests that the contribution of ^{127}I T_1 to the observed T_1 through this mechanism can be neglected in the present discussion.

In Eqs. 11 and 12, the self-diffusion of iodide ions expected to be possibly excited was assumed to be much slower than that of the cations, namely, $\tau_H \ll \tau_I$ by considering their large mass. Here, τ_I indicates the diffusion correlation time of the anion. Eqs. 11 and 12 were proved to be still valid by substituting $(\tau_H^{-1}+\tau_I^{-1})$ for τ_H^{-1}, even if τ_I becomes comparable to τ_H. Since the observed T_1 of the ε phase decreased with increasing temperature, the condition of $\omega_H\tau_H \gg 1$ is reasonably assumed to be fulfilled over the whole temperature range of this phase. Therefore, Eqs. 7, 8, 11, and 12 can be rewritten as,

$$T_{1HH}^{-1} = 4\alpha(S_0 - S_1/\bar{Z})/y, \tag{14}$$

$$T_{2HH}^{-1} = 3\alpha y g(0), \tag{15}$$

$$T_{1HI}^{-1} = \beta[(S_0' - S_1'/\bar{Z})/(\omega_H - \omega_I)^2 + (S_0' - S_1'/\bar{Z})/\omega_H^2 + 2(S_0' - S_1'/\bar{Z})/(\omega_H + \omega_I)^2]1/2\tau_H, \tag{16}$$

$$T_{2HI}^{-1} = 2\beta\tau_H g'(0), \tag{17}$$

where $\bar{Z}$ denotes the number of the nearest neighbors of the simple cubic sublattice. S_i and S_i' are defined in Sholl's paper.[29] Accordingly, the total relaxation rates, $T_{1\varepsilon}^{-1}$ and $T_{2\varepsilon}^{-1}$ determined for the protons of this phase are given by $(T_{1HH}^{-1}+T_{1HI}^{-1})$ and $(T_{2HH}^{-1}+T_{2HI}^{-1})$, respectively.

In Eqs. 14 and 15, S_0, S_1, and $g(0)$ can be calculated by regarding as that the protonic system assumed to be concentrated at the center of gravity of the cation forms a simple cubic sublattice, because the crystal has the CsCl type bcc structure. According to the Sholl paper,[29] he obtained S_0=8.4019, S_1= 11.5739, and $g(0)$=18.21. Using the numerical values evaluated by Sholl[29] for the simple cubic and bcc lattices, S_0', S_1', and $g'(0)$ in Eqs. 16 and 17 applicable to the system involving ^1H–^{127}I interactions were calculated to be 20.644, −3.470, and 32.7, respectively. Employing the following values, $a=4.86\times10^{-10}$ m and $\bar{Z}=6$, the total relaxation rates can be obtained as,

$$T_{1\varepsilon}^{-1} = \tau_H^{-1}[20.1\omega_H^{-2} + 0.43(\omega_H - \omega_I)^{-2} + 1.28\omega_H^{-2} + 2.56(\omega_H + \omega_I)^{-2}]\times10^8, \tag{18}$$

$$T_{2\varepsilon}^{-1} = 1.09\times10^9\tau_H. \tag{19}$$

Since ω_H/ω_I is approximately constant for the present case, it is evident from Eq. 18 that $T_{1\varepsilon}$ should be proportional to ω_H^2 at a constant temperature, and also the gradient of the log T_1 versus T^{-1} plot should be constant and independent of ω_H. However, the observed gradients of the log T_1 curves depend on ω_H employed and become gentle with increasing ω_H. Moreover, the ratio of ^1H T_1 observed at 20 and 42.5 MHz is T_1(20 MHz)/T_1(42.5 MHz)=0.36 in disagreement with the theoretical value of 0.22 derived from Eq. 18. These facts suggest that ^1H T_1 observed for the ε phase of MAI cannot be explained by the single relaxation mechanism of self-diffusion as dominantly concerned with.

Here, we introduce another assumption that two relaxation mechanisms appreciably contribute to ^1H T_1 of this phase and one of them involves ω_H whereas the other does not. For this case, the observed T_1 can be expressed by

$$T_1^{-1} = T_{1d}^{-1} + T_{1i}^{-1}, \tag{20}$$

where T_{1d} and T_{1i} represent ^1H T_1, which are proportional to ω_H^2 and independent of ω_H, respectively. Using Eq. 20, two components, T_{1d} and T_{1i}, were obtained from the observed T_1 values. The results are shown in Fig. 5. ^1H spin-rotation interaction already discussed in the α' phase can be proposed as the most probable relaxation mechanism for T_{1i} which decreases with increasing temperature. Because isotropic rotation of the cations is thought to be very rapid in this liquid-like ε phase, it will be the main origin of this mechanism.

The frequency dependent part T_{1d}, on the other hand, can be unequivocally assigned to the self-diffusion of the cations. The E_a value of 35 kJ mol^{-1} was obtained for this motional mode from the slope of the log T_{1d} curves of different ω_H. From the slope of the log T_2 versus T^{-1} curve, the same E_a value should be obtained as that derived above. However, a much larger E_a of ca. 48 kJ mol^{-1} was obtained from the log T_2 curve. Also for CH_3ND_3I, E_a derived from the log T_2 curve (45 kJ mol^{-1}) is much larger than that roughly evaluated from the log T_1 curve observed at 20 MHz (≈30 kJ mol^{-1}), although no accurate value could be determined because the T_1 data of CH_3ND_3I were obtained at only two ω_H.

In the preceding analysis of the relaxation times, we simply assumed that both T_{1d} and T_2 are determined through the same relaxation process. Referring to our T_1 and T_2 data observed in a fairly narrow temperature range without the location of T_1 minimum, the above assumption is not necessarily valid, because the origin of observed ^1H T_1 and T_2 cannot be definitely identified without the data in the temperature range where the condition $\omega_H\tau_H \leqq 1$ is satisfied. The fact that the different E_a values were derived from T_{1d} and T_2 suggests the existence of at least two different relaxation processes of self-diffusion.

As one of the relaxation models involving two kinds of self-diffusion processes, it is conceivable for the present ε phase that both cations and anions perform self-diffusion with different correlation times. For this model, τ_H and τ_I can be calculated from the above T_{1d} and T_2 expressions by replacing τ_H^{-1} with $(\tau_H^{-1}+\tau_I^{-1})$. The τ_I values calculated in the whole temperature range observed were negative. This is unreasonable result and, therefore, the above model is unacceptable for the present case.

As another possible model, it is considered that the cations diffuse through the activation of two kinds of self-diffusion mechanisms, i.e., local translational jumps among the adjacent small number of vacancy sites and a long-range self-diffusion mode where the cations migrate to a long distance through many vacancies as already considered for simple ionic conductors.[32] It is expected that the former process gives a shorter τ_H and a smaller E_a than the corresponding values in the latter. By applying this model to the present ^1H relaxation data, we can derive a conclusion that the relaxation process of T_{1d} is thought to be caused by the short-range self-diffusion whereas that of ^1H T_2 is governed by the long-range process.

The observed values of σ shown in Fig. 7 increase discontinuously by three orders of magnitude at T_{tr} to the ε phase. The large value of σ in this phase is attributable to ionic conduction of the diffusible cations, the existence of which is verified by the present NMR study. From σ values observed, we can evaluate the diffusion constant D_σ of the cations using the Nernst-Einstein equation written by

$$D_\sigma = kT\lambda\sigma/(Ze)^2N, \tag{21}$$

where Ze, N, and λ are the charge of diffusing ions, their number in a unit volume, and the spacial correlation factor calculated to be $\lambda=0.65331$ for the simple cubic lattice,[33] respectively.

The conductivity measurements in the ε phase gave E_a of 51 ± 3 kJ mol^{-1} which is larger than that derived from T_{1d}(31 kJ mol^{-1}) but close to that from ^1H T_2(48 kJ mol^{-1}). The fact that roughly the same value of E_a was obtained from σ and ^1H T_2 measurements suggests that the two different physical quantities are dominantly determined due to the same diffusion mechanism. In the present study, σ was measured by applying an ac electric field of 1 kHz. Since the transport distance, $\bar{r}_\sigma$ averaged in a time τ can be expressed by[34]

$$\bar{r}_\sigma = \sqrt{6D_0\tau}, \tag{22}$$

it can be shown that the long-range diffusion mainly contributes to σ, where ions migrate for longer distances than the order of 10^2 Å in a half cycle of 1 kHz. This gives a strong support for our previous conclusion about the process determing ^1H T_2.

The entropy changes at T_{tr}(414 K) and T_m of MAI crystals observed by DSC measurements were $\Delta S_{tr}=15$ J K^{-1} mol^{-1} and $\Delta S_m\approx14$ J K^{-1}mol^{-1}, respectively. These values can be compared with $\Delta S_{tr}=28$ J K^{-1} mol^{-1} and $\Delta S_m=12$ J K^{-1} mol^{-1} obtained for $CH_3NH_3NO_3$ crystals,[8] because the highest-temperature solid phase of both crystals is the liquid-like solid one. The fact MAI has ΔS_{tr} smaller than $CH_3NH_3NO_3$ crystal is understandable by considering that spherical iodide ions have no orientational freedom. Although ΔS_{tr} and ΔS_m values in MAI are comparable, the latter is unusually small as compared with that of usual ionic crystals such as NaSCN, KSCN, and KN_3. These salts[35] have ΔS_m of 30—40 J K^{-1} mol^{-1}. Usual molecular plastic crystals[36] are known to have ΔS_m less than ca. 20 J K^{-1} mol^{-1}. Accordingly, it is concluded that the cations in the ε phase are in a state having the most part of their motional freedom in good agreement with the foregoing conclusion derived from the present NMR and X-ray studies, and the ε phase can be considered as a plastic phase. A similar state of molecule-like cations can be found in the highest-temperature solid phase of NH_4NO_3,[37] $CH_3NH_3NO_3$,[7,8] $CH_3NH_3ClO_4$,[7] $(CH_3NH_3)_2SO_4$,[38] and $[C(NH_2)_3]ClO_4$.[39]

The authors are grateful to Prof. S. Kawai and Dr. K. Kitahama of Osaka University and Dr. Y. Furukawa for their help in carrying out the measurements of X-ray diffraction. We also wish to thank Mr. K. Kawase and Dr. K. Toriyama in the Government Industrial Research Institute of Nagoya for help in the experiments of DSC.

References

1) A. Cabana and C. Sandorfy, *Spectrochim. Acta*, **18**, 843 (1962).
2) A. Théorêt and C. Sandorfy, *Spectrochim. Acta, Part A*, **23**, 519 (1967).
3) S. B. Hendricks, *Z. Kristallogr.*, **67**, 106 (1928).
4) G. Jugie and J. A. S. Smith, *J. Chem. Soc., Faraday Trans. 2*, **74**, 994 (1978).
5) H. Ishida, R. Ikeda, and D. Nakamura, *Phys. Stat. Sol. (a)* **70**, K151 (1982).
6) C. S. Sandaram and J. Ramakrishna, *Current Science*, **51**, 835 (1982).
7) H. Ishida, R. Ikeda, and D. Nakamura, *Chem. Lett.*, 1943 (1982).
8) H. Ishida, R. Ikeda, and D. Nakamura, *J. Chem. Soc., Faraday Trans. 2*, **81**, 963 (1985).
9) O. Yamamuro, M. Oguni, and H. Suga, to be published.
10) L. S. Prabhumirashi, R. Ikeda, and D. Nakamura, *Ber. Bunsenges. Phys. Chem.*, **85**, 1142 (1981).
11) S. Gima, Y. Furukawa, R. Ikeda, and D. Nakamura, *J. Mol. Struct.*, **111**, 189 (1983).

12) E. L. Hahn, *Phys. Rev.*, **80**, 580 (1950).
13) Y. Kume, R. Ikeda, and D. Nakamura, *J. Magn. Reson.*, **33**, 331 (1979).
14) F. D. Rossini, D. D. Wagman, W. H. Evans, S. Levine, and I. Jaffe, Selected Values of Chemical Thermodynamic Properties Part I. Tables, NBS Circular 500-Part I, U. S. Goverment Printing Office, Washington (1961).
15) Y. Kume, R. Ikeda, and D. Nakamura, *J. Phys. Chem.*, **82**, 1296 (1978).
16) H. Ishida, R. Ikeda, and D. Nakamura, *J. Phys. Chem.*, **86**, 1003 (1982).
17) J. Tsau and D. F. R. Gilson, *Can. J. Chem.*, **48**, 717 (1970).
18) A. Abragam, "The Principles of Nuclear Magnetism," Oxford Univ. Press, Oxford (1961).
19) T. Nakagawa and Y. Koyanagi, Program library in Computation Center of Nagoya University, code number 466.
20) R. Ikeda, Y. Kume, D. Nakamura, Y. Furukawa, and H. Kiriyama, *J. Magn. Reson.*, **24**, 9 (1976).
21) Y. Furukawa, H. Kiriyama, and R. Ikeda, *Bull. Chem. Soc. Jpn*, **54**, 103 (1981).
22) R. Ikeda and C. A. McDowell, *Chem. Phys. Lett.*, **14**, 389 (1972).
23) F. Köksal and S. Bahceli, *J. Chem. Soc., Faraday Trans. 2*, **74**, 1844 (1978).
24) K. Simomura, M. Yoshida, A. Sanjoh, and H. Negita, *Phys. Lett.*, **81A**, 189 (1981).
25) P. S. Hubbard, *Phys. Rev.*, **131**, 1155 (1963).
26) H. W. Spiess, D. Schweitzer, and U. Haeberlen, *J. Magn. Reson.*, **9**, 444 (1973).
27) D. W. G. Smith and J. G. Powles, *Mol. Physics*, **10**, 451 (1966).
28) H. C. Torrey, *Phys. Rev.*, **92**, 962 (1953).
29) C. A. Sholl, *J. Phys. C*, **7**, 3378 (1974); **8**, 1737 (1975).
30) A. R. Sharp and M. M. Pintar, *J. Chem. Phys.*, **75**, 2652 (1981).
31) M. O. Norris, J. H. Strange, J. G. Powles, M. Rhodes, K. Marsden, and K. Krynicki, *J. Phys. C* **1**, 422 (1968).
32) P. M. Richards, "Magnetic Resonance in Superionic Conductors," and T. Geisel, "Continuous Stochastic Models," in M. B. Salamon Ed., "Physics of Superionic Conductors," Springer-Verlag, Berlin, (1979), p. 141 and p. 202, respectively.
33) K. Compaan and Y. Haven, *Trans. Faraday Soc.*, **52**, 786 (1956); **54**, 1498 (1958).
34) J. M. Chezeau and J. H. Strange, *Phys. Rep.*, **53**, 1 (1979).
35) G. J. Janz, "Molten Salts Handbook," Academic Press, N. Y. (1967).
36) J. Timmermans, *J. Phys. Chem. Solids*, **18**, 1 (1961).
37) M. T. Riggin, R. R. Knispel, and M. M. Pintar, *J. Chem. Phys.*, **56**, 2911 (1972).
38) H. Ishida, T. Matsuhashi, R. Ikeda, and D. Nakamura, *Chem. Lett.*, **1985**, 1859.
39) S. Gima, Y. Furukawa, and D. Nakamura, *Ber. Bunsenges. Phys. Chem.*, **88**, 939 (1984).